High-resolution mass spectrometry and nontraditional mass defect analysis of brominated historical pigments

High-resolution mass spectrometry and non-traditional mass defect analysis of brominated historical pigments

Alba Alvarez-Martin[1,2,3*], G. Asher Newsome[2], Koen Janssens[1]

[1]AXIS, NANOLab Centre of Excellence, Department of Physics, University of Antwerp, 2020 Antwerpen, Belgium

[2]Smithsonian Institution, Museum Conservation Institute, 20746 Suitland MD, USA

[3]Conservation and Science, Rijksmuseum Amsterdam, 1071 ZC Amsterdam, The Netherlands

*Corresponding author: Alba.AlvarezMartin@uantwerpen.be

GRAPHICAL ABSTRACT

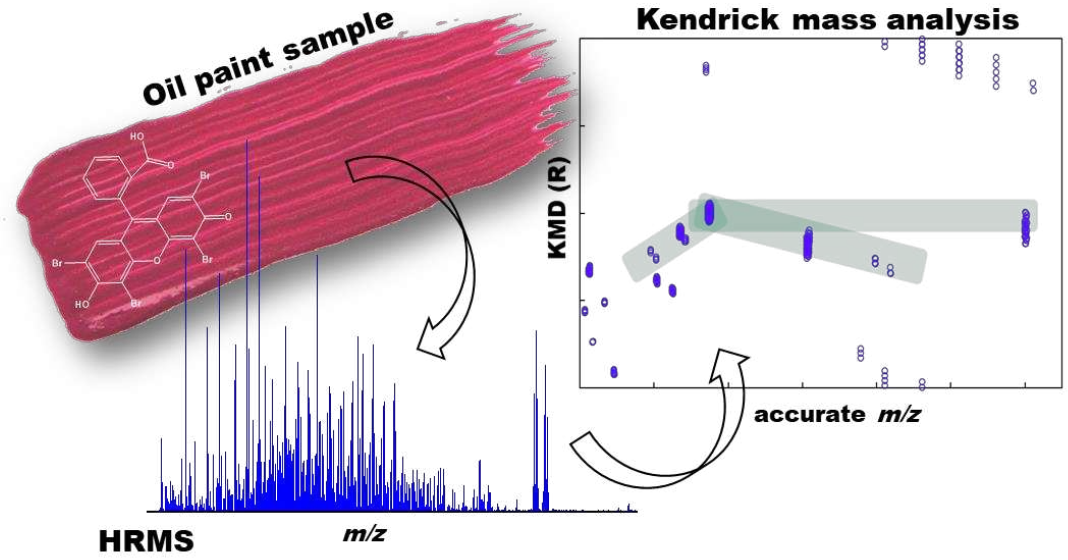

ABSTRACT

The implementation of high-resolution mass spectrometry (HRMS) systems offers new possibilities for the analysis of complex art samples such as historical oil paintings. However, these multicomponent systems generate large and complex datasets that require advanced visualization tools to aid interpretation, especially when no chromatographic separation is performed. In the context of this research, it was crucial to propose a data analysis tool to identify the products generated during the synthesis, drying and aging of historical pigments. This study reports for the first time a non-traditional mass defect analysis of oil paint samples containing a fugitive brominated-organic pigment, eosin or geranium lake, by using direct infusion electrospray ionization in combination with a high-resolution Orbitrap mass spectrometer. The use of non-traditional Kendrick mass defect plots is presented in this study as a processing and visualization tool to recognize brominated species based on their specific mass defect and isotope pattern. The results demonstrate that this approach could provide valuable molecular compositional information on the degradation pathways of this pigment. We anticipate that mass defect analysis will become highly relevant in future degradation studies of many more historical organic pigments.

INTRODUCTION

The fast advances in organic chemistry during the 19th century resulted in the discovery of new compounds and chemical reactions. These discoveries not only had an impact on the quality of life but also had a direct impact in the palette of oil painters and watercolourists, due to the synthesis of new organic pigments and their rapid manufacture and commercialization as paint tubes.

In recent years one of these new synthetic pigments, eosin lake (historically sold as geranium lake), was identified for the first time in the oeuvre of Gauguin and van Gogh.[1] Historical geranium lake recipes describe the precipitation of the eosin dye (Figure SI.1) onto aluminium or lead salts to form an insoluble pigment.[2] The result is an aggregate of eosin molecules complexed to the metal substrate.[3,4] However, eosin lakes were originally manufactured for lithography, book and wallpaper printing, and not for easel painting. Despite its brightness and beautiful hue, from purple to pink, this family of brominated pigments tends to rapidly fade leading to the discoloration of masterworks within an artist's lifetime[1,5] and makes identification in the artwork very challenging. This is because eosin is a photosensitizer,[6,7] and its degradation mechanism is therefore strongly affected by the presence of light and oxygen,[8] and surrounding media. For example, the detection of bromine, an element rarely found in historical pigments, by scanning electron microscopy-energy dispersive X-ray spectrometry (SEM−EDS) and macroscopic X-ray fluorescence (MA-XRF) analysis has been hypothesized to indicate the presence of eosin on van Gogh's paintings.[9,10] However, the identification of geranium lakes in original paintings by chromatographic techniques has relied solely on the detection of the intact eosin chromophore.[11,12]

A series of recent publications focused on the detection of geranium lakes by mass spectrometry have contributed very significantly to this research topic.[13-15] Nevertheless, the side-products formed during the synthesis of geranium lakes, as well as their degradation mechanisms in oil

53 paintings, are still unclear. In addition, it has been observed that the metal used to complex the
54 eosin could affect the lightfastness due to the molecular structure of the lake.[4,16] However, up to
55 now, no mass spectrometric analysis has been performed to reach a deeper understanding of the
56 possible degradation process of the different metallic complexes.
57 In our previous study we proposed a breakdown technology in the field of conservation science
58 exploring direct analysis in real time (DART) and direct infusion electrospray ionization (DI-ESI)
59 coupled to high resolution mass spectrometry (HRMS) for chemical identification of these
60 brominated historical pigments in oil paints.[15] However, the interpretation of HRMS datasets
61 obtained by direct analysis in real time and by direct infusion can be challenging due to the large
62 amount of information generated. At the same time, geranium lake-oil paints may contain a
63 complex mixture of related brominated products associated with impurities, due to the synthesis
64 conditions and/or interaction with the binding media, and degradation products formed over time.
65 Data analysis generated by the HRMS system is simplified here using the fact that geranium lakes
66 have a unique mass defect (i.e., the difference between the exact and the nominal mass) and a
67 discrete isotopic pattern, which readily distinguishes them from non-brominated species in a
68 complex mass spectrum. A large range of visualization strategies based on the resolution and mass
69 defect information offered by HRMS are available to mitigate the effects of the matrix interference
70 and improve the identification of target compounds.[17]
71 A common strategy to track repeating units in polymeric materials was proposed by Kendrick in
72 1963.[18] Kendrick mass (KM) analysis is based on arbitrarily setting the mass of the CH_2 unit to
73 14, instead of its IUPAC mass (m(CH_2)=14.01565). The IUPAC mass of a repeating unit can then
74 be converted to the Kendrick mass (KM) as:
75 $$KM=m/z*(14/14.01565).$$

The Kendrick mass defect (KMD) is the difference between the rounded KM and the exact KM:

$$KMD=round(KM)-KM.$$

This approach facilitates the visualization of a homologous series of compounds that share the same mass defect when plotting their KMD as a function of m/z.

In the literature, Kendrick analysis has been extended to non-polymeric samples by selecting the exact mass of an appropriate rescaling unit (R).[19] In this case, the rescaled Kendrick mass (KM(R)) is calculated as:

$$KM(R)=m/z*round(R)/R.$$

As before, the corresponding KMD (aka Rescaled Kendrick mass) can be calculated as:

$$KMD(R)=round(KM(R))-KM(R).$$

Recently, it has been shown that this new approach is a suitable method for the analysis and chemical fingerprint of halogenated compounds.[20] By using non-traditional rescaling units such as -H/+Cl, CF_2, +F/-Cl, -HBr, the plot can act help analysts to visually separate homologous (halogenated) series that are not so easy distinguishable in the original mass spectrum.[21-23]

In this study, a non-traditional Kendrick mass analysis, based on the concept of rescaling units, has been successfully applied for first time on a series of historical brominated-organic pigments. Oil paints prepared from two different metallic conformations of geranium lake, observed in van Gogh paintings [1], aluminium (Al^{3+}) and lead (Pb^{2+}) based, were analysed by DI-ESI-HRMS with the aim of detecting brominated impurities, side-products coming from the synthesis, and degradation products formed during the drying and aging of the oil paint.

MATERIAL AND METHODS

Chemicals

Eosin-Y (99% dye content) was purchased from Sigma-Aldrich. Aluminium chloride hexahydrate ($AlCl_3 \cdot 6H_2O$) was purchased from Fluka. Lead (II) acetate trihydrate ($Pb(CH_3CO_2)_2 \cdot 3H_2O$) was purchased from Merck. The bleached linseed oil (Talens) employed to prepare the paints was diluted with turpentine (Winsor & Newton).

Synthesis of geranium lakes, oil paint samples preparation and artificial photoaging

The synthesis of the eosin-based, or geranium, lakes was carried out according to the protocol proposed by Claro et al.[3] Oil paint models were prepared by mixing each of the metallic lakes with linseed oil and painting them out on glass slides; paint films of approximately 100 μm thickness were obtained in this manner. The final oil paints were kept in the dark for 4 weeks at 20 °C and at environmental humidity (about 60% RH). Oil paint samples were subjected to accelerated light aging up to 553 h in a controlled climate chamber (Model UV 200RB/20DU, Weiss Technik) equipped with a UVA (350−400 nm) lighting system (Actinic BL TL, Philips). The temperature (21 °C) and relativity humidity (30%) were kept constant during the photoaging.

Studied samples

Powder samples of both metallic lakes (aluminium- or lead-eosin based) were kept in the dark until the analysis and were considered as reference materials, i.e., without the presence of linseed oil and without artificial aging. For this study, the oil paint samples corresponding to time 0 h (unaged) and 553 h (aged) were analysed to monitor the change experienced during: (1) the drying process (unaged oil paint sample) and (2) artificial aging (aged oil paint sample). Here it is important to note that unaged paint samples were also kept in the dark until the analysis.

DI-ESI-HRMS analysis

The extraction protocol was followed as described in our previous publication.[15] Solvent extract was infused at 10 μL/min and electrosprayed into an LTQ Orbitrap Velos mass spectrometer. High-resolution MS1 and MS2 were acquired in positive mode (m/z 150−2000) at 30000 resolving power. For tandem mass analysis, each selected analyte was isolated with a 4 m/z window for 0−45% collision energy (CE) for collision induced dissociation (CID) and 0−45% normalized collision energy (NCE) for higher-energy collisional dissociation (HCD). The background subtraction of the solvent was performed during data analysis.

RESULTS

Characterization of historical geranium lakes

Geranium lakes are constituted by an aggregate of eosin molecules complexed to an inorganic substrate. Unaged powder samples of aluminium- and lead-based eosin lakes were studied in this section as reference materials to identify the eosin:metal complex (aka lake) and to evaluate the possible formation of side-products generated during the synthesis.

The presence of a heteroatom such as Br, present not only in the lake, but also in the side-products, produced a rich and specific isotopic pattern that makes the evaluation of the mass spectrum more complicated (Figure SI.2). To simplify the identification of the native conformation of geranium lake, we selected the mass of the most abundant isotope of a single tetra-brominated eosin molecule, ($[C_{20}H_9O_5{}^{79}Br_2{}^{81}Br_2]^+$, abbreviated as $EoBr_4$), as a base unit (R= 648.7132). The advantages of choosing the most abundant isotope, over the monoisotopic mass, for mass rescaling and the nature of its impact on point alignments in Kendrick analysis have been already discussed to track brominated flame retardants.[24]

A pattern of brominated species can be visually recognized in the non-traditional Kendrick plot or rescaled KMD plot of the aluminium and lead-based lakes (Figure 1). These plots show a horizontal alignment of brominated species differing along the *m/z* axis by the repeating unit (in this case a tetra-brominated eosin, $EoBr_4$). Because they have the same mass defect, for both Al-eosin and Pb-eosin lakes, the 2:1 (eosin:metal) complexes ($EoBr_4$-Al-$EoBr_4$ at *m/z* 1318.4069 ($[C_{40}H_{12}{}^{79}Br_4{}^{81}Br_4O_{10}Al]^+$) and $EoBr_4$-Pb-$EoBr_4$ at m/z 1502.3843 ($[C_{40}H_{15}{}^{79}Br_4{}^{81}Br_4O_{10}Pb]^+$)), can also be identified in this horizontal line. In the mass spectrum of both metallic lakes, it can been seen that next to the 2:1 (eosin:metal) complex also the doubly charged tetramer form (2[$EoBr_4$-M-$EoBr_4$]) is observed (Figure SI.3). The mass spectrum of the lead-based lake also shows a larger lead complex at *m/z* 1707.3408, which correspond to the doubly charged 2:2 (eosin:metal) complex ($[C_{40}H_{14}{}^{79}Br_4{}^{81}Br_4O_{10}Pb_2]^{2+}$) (Figure SI.4). The doubly charged species detected in both lakes, indicate that larger structures can be formed beside the 2:1 eosin:metal complex reported up to now.[3,4] In addition, the difference between the exact m/z of the aluminium complex detected in this study and what is reported by Anselmi shows that eosin molecules can show different coordination modes in presence of aluminium.

However, other brominated species that do not contain the repeating unit ($EoBr_4$) appear with an oblique alignment relative to the tetra-brominated forms in Figure 1. As these species are already observed in the lake powder studied in this section, they can be considered as side-products formed during the synthesis and will be discussed in the next section.

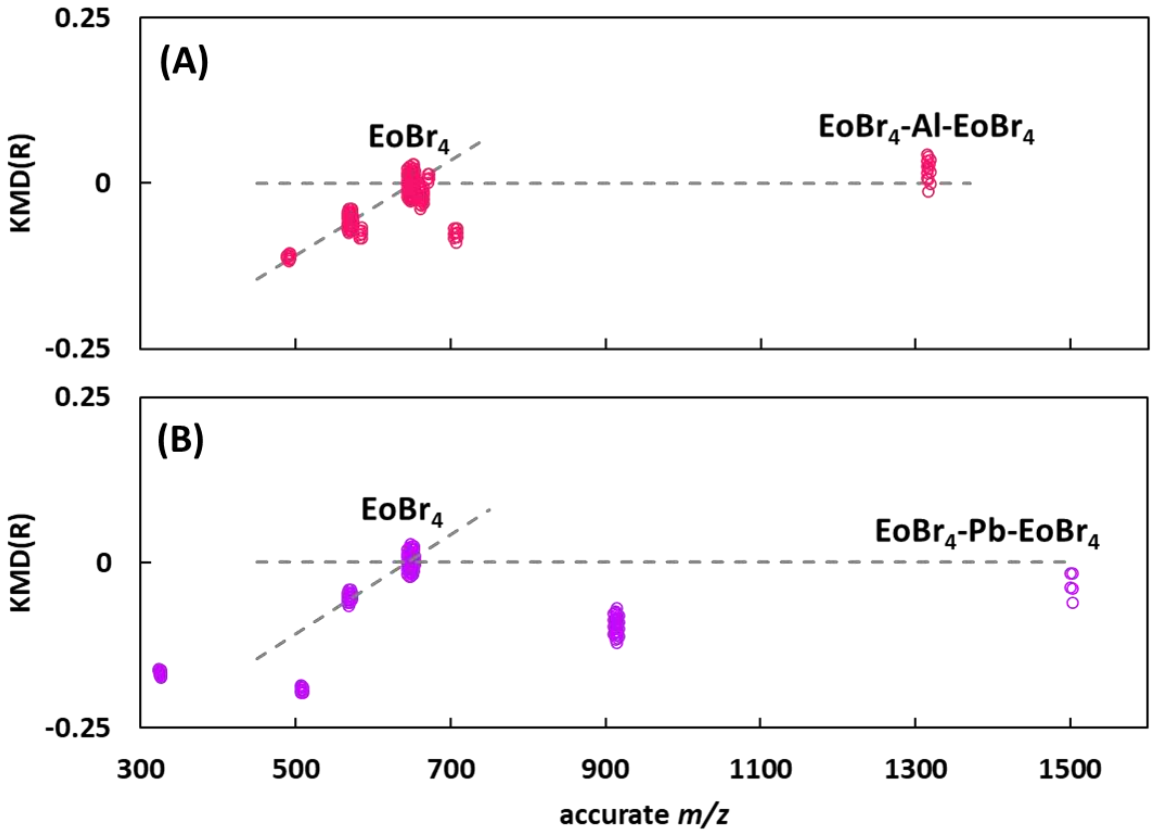

Figure 1. Rescaled Kendrick plots of (A) aluminium-based and (B) lead-based eosin lakes using the most abundant isotope of the repeating unit of EoBr4 (R=648.7132).

Evaluation of side-products generated during the synthesis

The first approach to identify in Figure 1 the brominated species that appear with an oblique alignment regarding the tetra-brominated form ($EoBr_4$) was to consider the monoisotopic mass of bromine (^{79}Br) as the base unit (R=78.9183) for Kendrick mass analysis. This aims to visually identify compounds correlated by subsequent addition or subtraction of bromine atoms. Surprisingly, the resulting rescaled or non-traditional Kendrick plot (Figure 2A and SI.5A) displays several point series with oblique alignments, indicating that the bromine atom is not the only difference between these compounds. Secondly, the scale factor -HBr (R=79.9262) was then

used as a new base unit. However, in the resulting mass defect plots, the tangential alignment indicated that the loss of HBr (or dehydrobromination) did not explain the difference between adjacent compounds (Figure 2B and SI.5B). The third variation consisted in setting the scale factor to −Br+H (R=77.9105), obtaining the instant rotation of the mass defect plot until the series are clearly aligned horizontally (Figure 2C and SI.5C). This confirms that one of the side reactions occurring during synthesis is the loss of a radical Br·, which is replaced by a H· radical (debromination). The use of this base unit clearly facilitates the rapid identification of brominated side-products generated during the synthesis of the aluminium- and lead-based lakes (Table SI.1 and SI.2). In Figure 2C (aluminium-based lake) two compounds, with horizontal alignment regarding the tetra-brominated form and differing by the number of bromine substituents, can be identified as tri- and di-brominated eosin forms ($EoBr_3$ and $EoBr_2$ at m/z 568.8056 ($[C_{20}H_{10}O_5{}^{79}Br_2{}^{81}Br]^+$) and 490.8949 ($[C_{20}H_{11}O_5{}^{79}Br{}^{81}Br]^+$), respectively). Simultaneously, the presence of other brominated species with oblique alignments regarding the tetra-, tri- or di-brominated forms in the unaged aluminium-based lake (Figure 2C) indicates the formation of other compounds associated to these species. The clusters at *m/z* 584.8192 ($[C_{21}H_{12}O_5{}^{79}Br_2{}^{81}Br]^+$) and *m/z* 662.7296 ($[C_{21}H_{11}O_5{}^{79}Br_2{}^{81}Br_2]^+$) correspond to the methylated forms of $EoBr_3$ and $EoBr_4$ eosin, respectively ($EoBr_3$+Me and $EoBr_4$+Me).[13,15]

Other two species associated to the tetra-brominated form at *m/z* 706.7683 ($[C_{23}H_{15}O_6{}^{79}Br_2{}^{81}Br_2]^+$, $EoBr_4$-Ester) and at *m/z* 670.6949 ($[C_{20}H_4O_5{}^{79}Br_2{}^{81}Br_2Al]^+$, $EoBr_4$+Al) were also identified.

After applying the scale factor −Br+H (R=77.9105) to the unaged lead-based powder lake, the only compound with a horizontal alignment regarding $EoBr_4$ was the tri-brominated form ($EoBr_3$) (Figure SI.5C). In contrast to the case of the aluminium-eosin complexes discussed above, no other brominated species were visible about the detection limit of the method. Furthermore, no

methylated or ester derivatives were identified in the lead-based lake. However, a single species at *m/z* 329.0048, not detected in the aluminium-based lake, and yet unidentified is observed in Figure SI.5C.

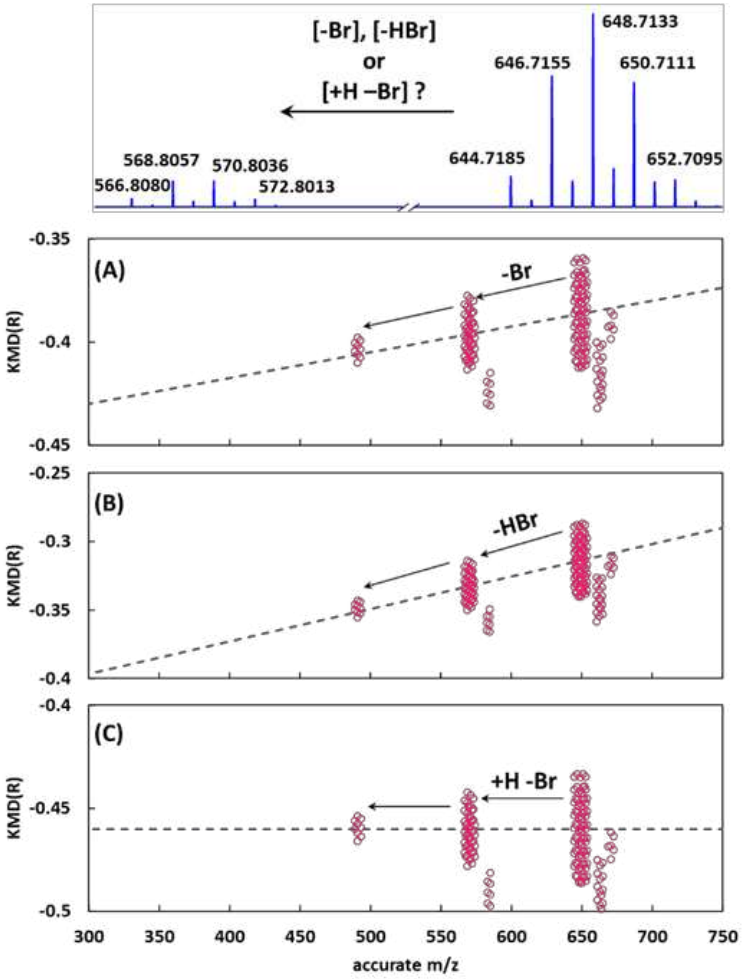

Figure 2. Rescaled Kendrick plot of the aluminium-based eosin lake using: (A) 79Br as the base unit (R=78.91833), (B) -HBr as the base unit (R=79.9262) and (C) −Br+H as the base unit (R=77.91051).

Monitoring of geranium lake markers during the drying and aging of oil paints

The abundance of all original (i.e., present in the powders) and newly formed species were monitored in the oil paint samples during drying and artificial aging (Table SI.1 and SI.2).

As described in the previous section, by using -H+Br (R=77.9105) as the rescaling unit, three horizontally aligned species, corresponding to tetra- tri- and di-brominated eosin, were observed in the unaged aluminium-based powder lake (Figure 3A). At the moment that the aluminium-based lake was mixed with linseed oil, the mono- and non-brominated species (EoBr at *m/z* 412.9836 ($[C_{20}H_{12}O_5Br]^+$) and fluorescein at *m/z* 333.0755 ($[C_{20}H_{13}O_5]^+$)) became readily visible in the rescaled Kendrick plot (Figure 3B and C).

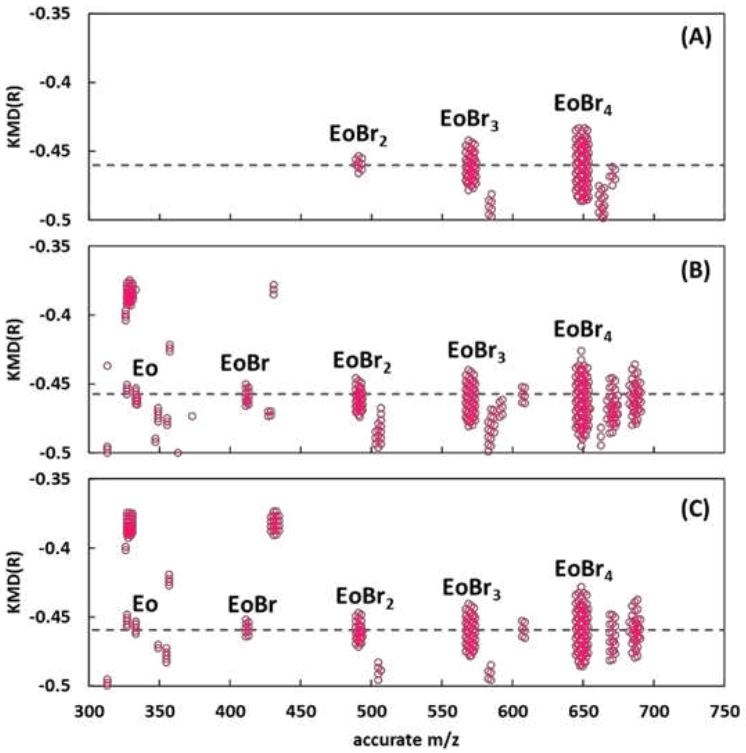

Figure 3. Rescaled Kendrick plot of the aluminium-based eosin lake using −Br+H as the base unit (R=77.9105) of: (A) unaged powder lake, (B) unaged oil paint and (C) aged oil paint.

By monitoring the abundance in the oil paints of these four brominated species, plus fluorescein (in the graph as $EoBr_0$) (Figure 4), it is clear that the debromination process, already detected during the synthesis, continues to take place during the drying and aging of the oil paints. As it can

be observed in Figure 4, the abundance of the tetra-brominated species decreased, while all other debrominated species increased during the drying and photoaging of the oil paint. It is interesting to note here that mono-brominated and non-brominated eosin (or fluorescein) were not detected in the unaged lake powder, indicating that these species already begin to be generated during the drying process of the oil, and their abundance further increases under irradiation with light. These results are consistent with our previous study, where we described the generation of debrominated species during the artificial aging of oil paint samples by DART-MS.[15]

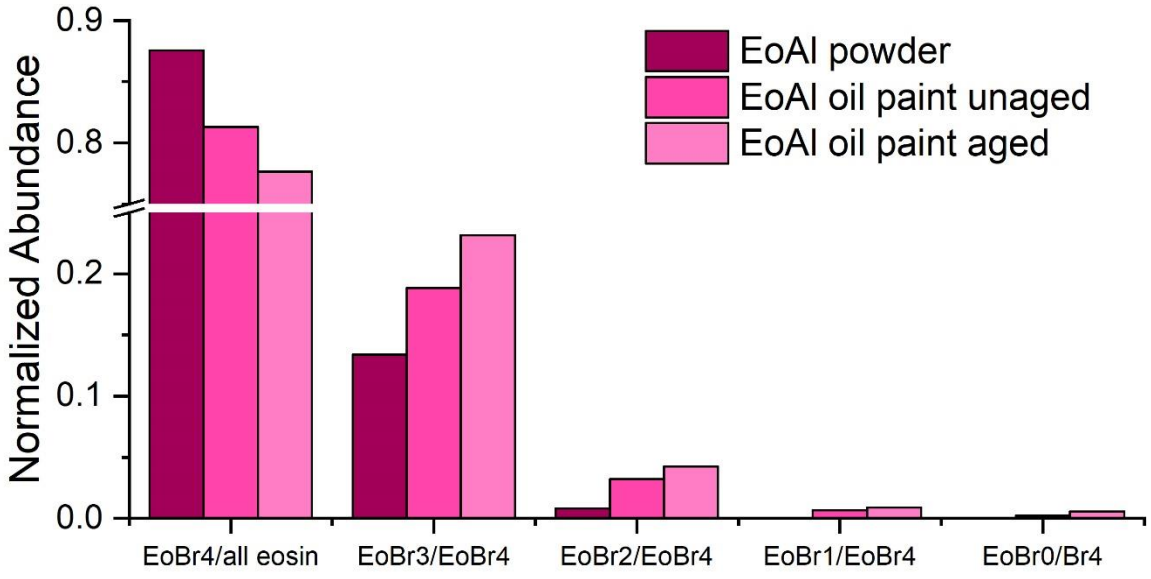

Figure 4. Abundance ratio of brominated products identified in the aluminium-based eosin lake in powder lake, unaged oil paint and aged oil paint.

In addition, the Kendrick plots of the oil paint samples (Figure 3B and C) show two new clusters, at *m/z* 504.9106 ($[C_{21}H_{13}O_5{}^{79}Br^{81}Br]^+$) and *m/z* 686.6701 ($[C_{20}H_4O_6{}^{79}Br_2{}^{81}Br_2Al]^+$), associated with the methylated form of $EoBr_2$ ($EoBr_2$+Me) and with the oxidation form of the $EoBr_4$+Al ($EoBr_4$+Al+O).The visual differences observed between the Kendrick plots of the powder pigment

(Figure 3A) and the oil paint samples (Figure 3B-C) can be confirmed by monitoring the abundance of the exact m/z during drying and aging. For example, the abundance of the di- and tri-methyl derivatives ($EoBr_2$+Me and $EoBr_3$+Me) slightly increases when the lake powder is mixed with linseed oil (Figure 5A). However, the abundance of $EoBr_4$+Me is substantially reduced after being in contact with the oil (Figure 5A). These trends can be linked to the abundance of their non-methylated species during drying and aging in Figure 4, where the di- and tri-brominated forms increased but the tetra-brominated form decreased.

However, the ester derivative form of $EoBr_4$ and the two fragments containing aluminium ($EoBr_4$+Al and $EoBr_4$+Al+O) clearly increase during the drying and aging of the oil paints (Figure 5B) probably due to the breakdown of the 2:1 (eosin:aluminium) complex and its further oxidation in presence of linseed oil.

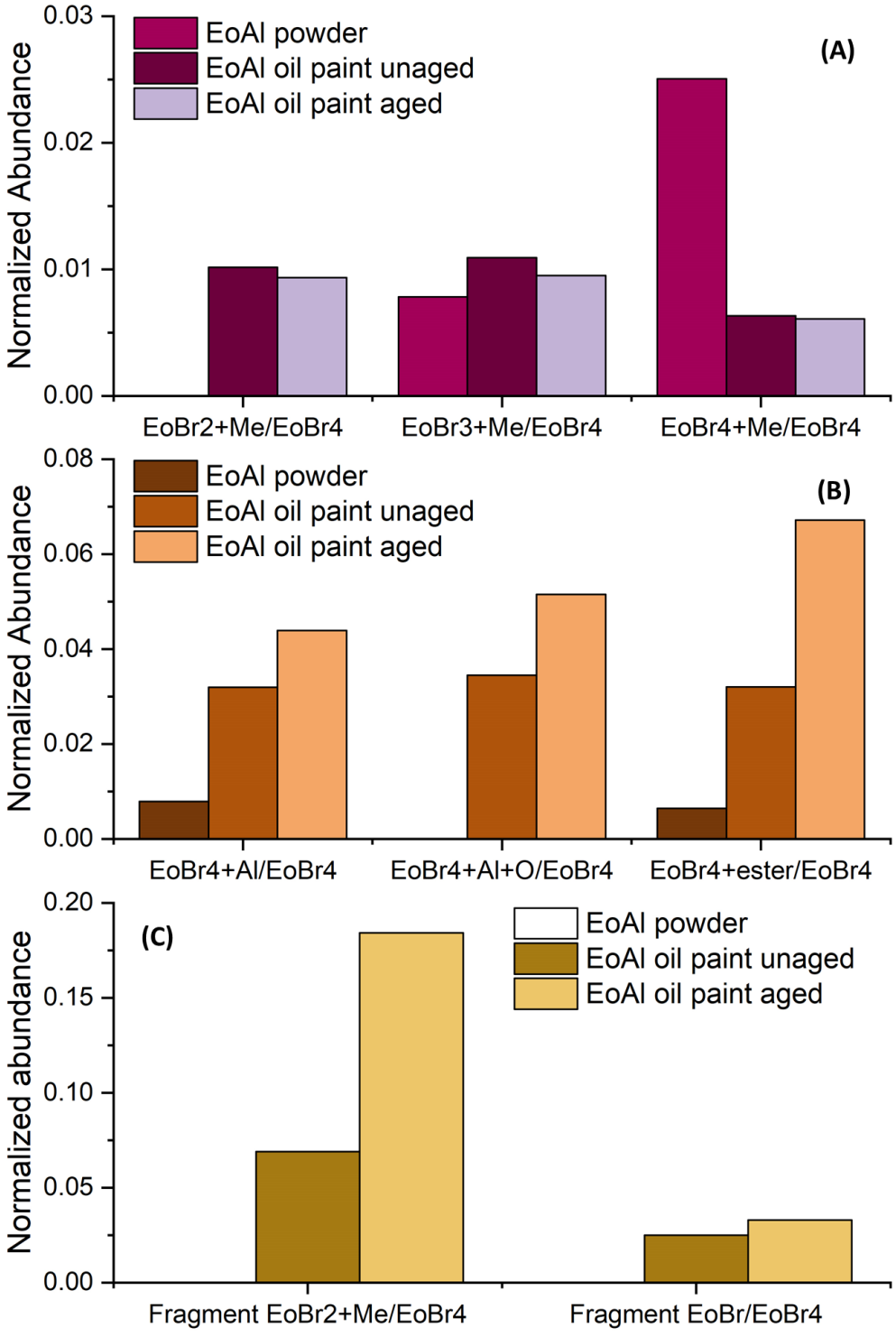

248

249 **Figure 5.** Abundance ratio of geranium aluminium-based lake markers identified in unaged
250 powder lake, unaged oil paint and aged oil paint. (A) methyl derivatives, (B) markers containing
251 aluminium and (C) fragments after chromophore breakdown.

Figures 3B and C also indicate the presence of two new compounds in the oil paints with oblique alignments regarding the di- and mon-brominated forms. The form at *m/z* 430.8875 ($[C_{15}H_{11}O_5{}^{79}Br^{81}Br]^+$) corresponds to the fragmentation of the di-brominated eosin chromophore and further methylation of the carboxylic group (Figure SI.6).[13,25] The second eosin fragment is observed at *m/z* 329.0048 and might be associated to the fragmentation of the mono-brominated eosin ($[C_{16}H_8O_3{}^{79}Br]^+$). The extraction and further monitoring of the abundance associated with these two fragments indicates that they form only when the lake pigment is mixed with linseed oil and increase with the aging (Figure 5C).

When -H+Br (R=77.9105) was used as the rescaling unit for the lead-based oil paints, none of the side-products detected in the aluminium lakes were visible in the Kendrick plots of the lead-based samples (Figure 6). Only the species at *m/z* 430.875 and at 329.0048, associated with the fragmentation of the chromophore, were visible in the Kendrick plot of the oil paints. The tracking of these fragments also showed an increase in abundance during the aging of the oil paint (Figure SI.7A).

The cluster observed at *m/z* 914.6973 in Figure 1B corresponding to $[C_{22}H_{11}O_7{}^{79}Br_2{}^{81}Br_2Pb]^+$ ($EoBr_4$+Pb) has been also tracked during the drying and aging (Figure SI.7B). The decrease of the abundance of this specie confirms that it is an intermediate form generated during the synthesis of the lead-base geranium lake, and not a breakdown product of the eosin:lead complex.

By monitoring the brominated forms, it is also clear that the lead-based lake follows the same debromination pattern as the aluminium-based lake (Figure SI.8).

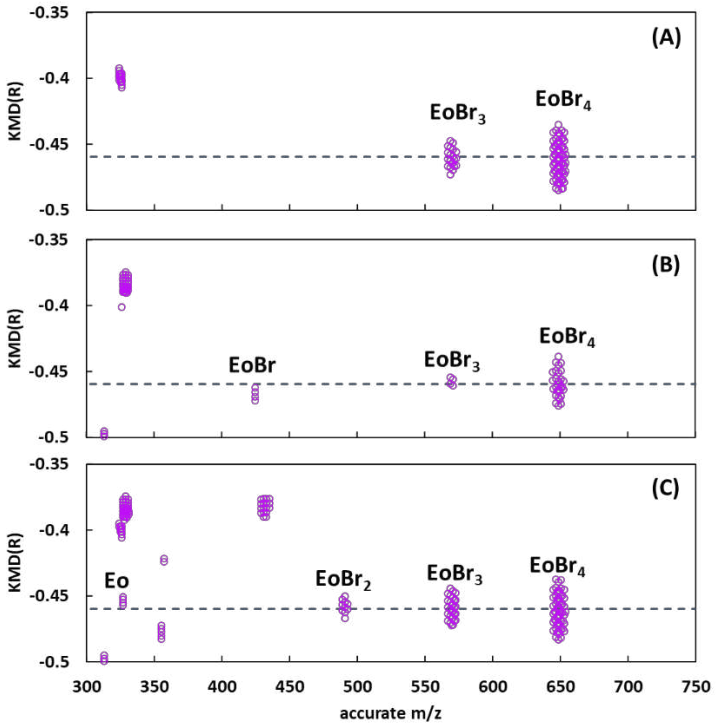

Figure 6. Rescaled Kendrick plot of the lead-based eosin lake using −Br+H as the base unit (R=77.9105) of: (A) unaged powder lake, (B) unaged oil paint and (C) aged oil paint

Monitoring of geranium lake complex during the drying and aging of oil paints

The 2:1 (eosin:aluminium) complex ($EoBr_4$-Al-$EoBr_4$ at *m/z* 1318.4069 ($[C_{40}H_{12}{}^{79}Br_4{}^{81}Br_4O_{10}Al]^+$) was monitored along the drying and aging of the oil paints. Figure 7 shows a decrease in abundance of the complex, indicating the breakdown of the eosin-aluminium bonds. Nevertheless, an increase in the abundance of the species derived from the 2:1 complex takes place during aging (Figure 7). These species are formed by the debromination of the 2:1 complex ($[C_{40}H_{13}{}^{79}Br_4{}^{81}Br_3O_{10}Al]^+$ at m/z 1240.4971),oxidation ($[C_{40}H_{12}{}^{79}Br_4{}^{81}Br_4O_{11}Al]^+$ at m/z 1334.3775) or both mechanisms ($[C_{40}H_{13}{}^{79}Br_4{}^{81}Br_3O_{11}Al]^+$ at m/z 1254.4699) (Figure SI.9 and Table SI.1). Interestingly, no 2:1 (eosin:lead) complex or derivatives were detected once the powder was mixed with the oil.

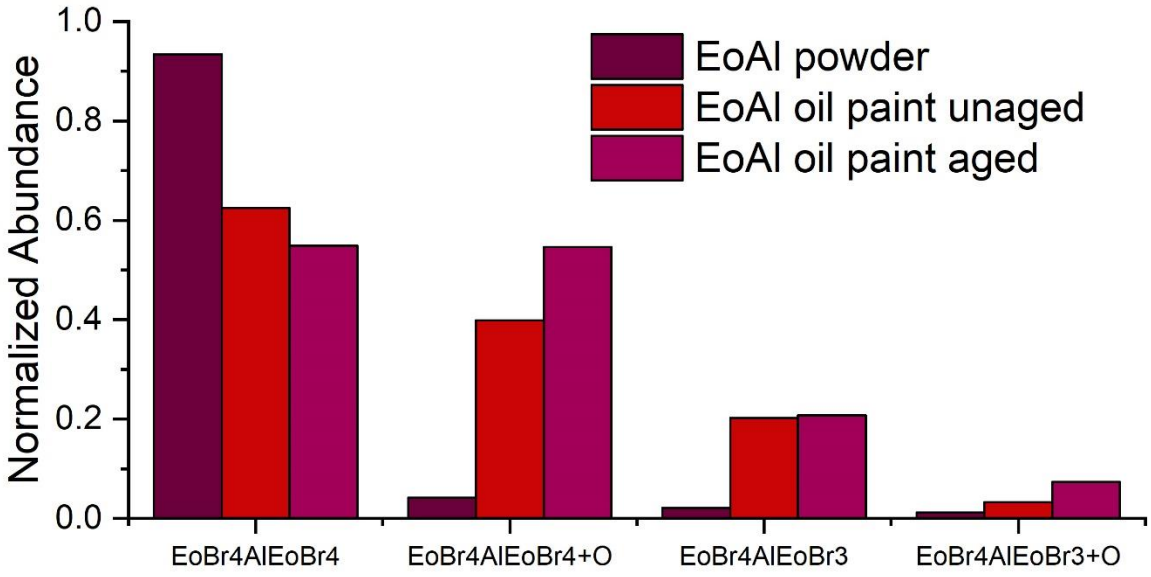

Figure 7. Abundance ratio of the metallic complex (eosin: aluminium) and derivatives identified in powder lake, unaged oil paint and aged oil paint.

Finally, MS/MS analysis carried out to confirm the different stability between the aluminium- and lead-based lakes revealed a significantly different fragmentation pattern for both metallic complexes, visible even with very low product ion abundance. The aluminium complex shows a fragmentation peak at *m/z* 672 which likely corresponds to the fragment $EoBr_4$-Al ($[C_{20}H_5O_5{}^{79}Br_2{}^{81}Br_2Al]^+$) already detected in the powder lake. In the case of the lead complex two fragmentation peaks (at *m/z* 639 and 676) are present. As the intensities of the obtained fragment ions are relatively low, additional experiments could be performed to optimize the fragmentation conditions of these species. These results indicate the difference in fragmentation pattern between aluminium and lead-based lakes, where both complexes open in different ways (Figure SI.10). The slightly different behaviour among aluminium- and lead-based lakes observed during the aging of the oil paints can be linked to the different conformations of the two lake complexes.[16]

303 *DISCUSSION*

304 The information obtained by mass defect analysis of HRMS data allows one to propose a
305 degradation scheme of the main molecular changes that geranium lakes undergo during aging
306 (Scheme 1).

307 Although it is the breakdown of the chromophore moiety that causes the total discoloration of the
308 eosin, we confirm here that geranium lakes present a tendency to lose bromine when the lake is in
309 contact with linseed oil in the presence of light and oxygen. Previous studies have proposed a
310 radical-mediated start of the reaction followed by oxidative debromination of the eosin molecule
311 and the production of high energetic $^1O_2$. The latter species will break the eosin chromophore. Two
312 breakdown products of the chromophore have been detected in this study (Scheme 1 and Tables
313 SI.1 and SI.2), however any smaller fragments due to further cleavage remain unidentified.

314 We also show that the metal used to complex the lake (Scheme 1A for aluminium and 1B for lead)
315 influences the reactivity occurring during the aging, which may be correlated with the literature
316 describing the different conformations and reactivity of geranium lakes.[4]

317 The methyl and ester derivatives, mostly detected in the aluminium lake (Scheme 1A), could be
318 produced during the synthesis due to the interaction with the solvent.[13,26,27] The photochemical
319 behaviour of eosin in different environments has been deeply investigated showing that its
320 complex protolytic system may easily react with the surrounding media.[28-30] As a result, the
321 formation of methylated and ester intermediates observed in this study is explained by the higher
322 acidity of the carboxylic group compared to the phenolic group due to the presence of bromine
323 groups. The negative charge of the basic form better stabilizes in the carboxylate than in the
324 phenolate, keeping the chromophore moiety intact.[26] However, since the monitoring of these
325 compounds indicates that the abundance increases with aging, their formation can also be

associated with the interaction with the oil matrix.[31] This proves that the reaction pathways involved in the discoloration of geranium lakes are much more than those described in the literature. The data obtained here suggests that esterification can also occur due to interaction with the oil in presence of light. In this case, the anchoring of the eosin to the metal through the carboxylic group will determine the chemoselective methylation and esterification reactions. This hypothesis confirms the different reactivity observed in the two metallic conformations studied here.

Finally, Kendrick mass analysis allowed visual detection of larger complexes that have not been described before in the literature, such as 2:2 eosin:metal complexes (in the case of the lead-based lakes) and oxidation products (in the aluminium-based lakes). These products indicate that the lakes not only undergo the breaking of bonds but also their functional groups can react to form bigger clusters.

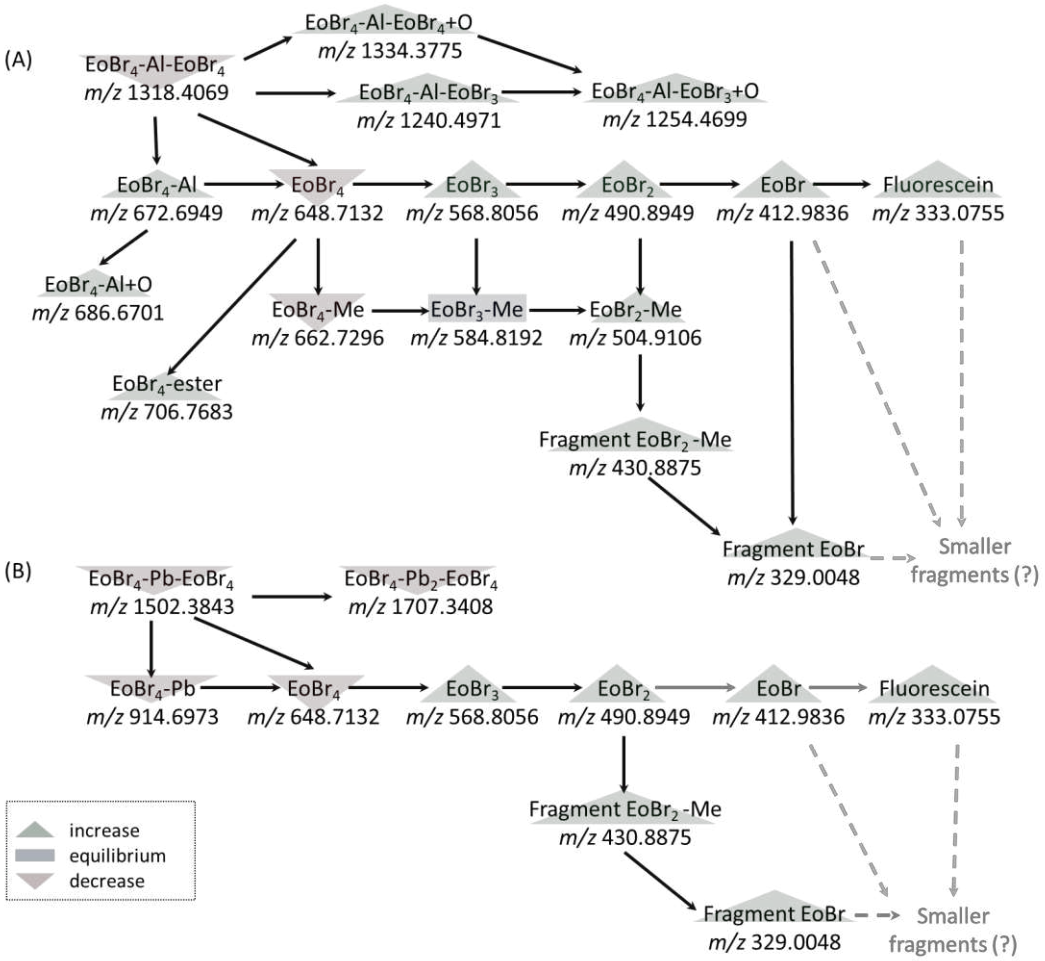

Scheme 1. Tentative fragmentation pathways of: (A) aluminium- and (B) lead-based geranium lakes. See Table SI.1 and SI.2 for more information about the compounds.

CONCLUSIONS

Non-traditional Kendrick mass analysis has been evaluated for the first time as a visualization tool to identify species associated with fugitive geranium lakes in oil paint samples. The approach proposed here is based on the detection of brominated products, either produced during the synthesis of the eosin pigment or formed as degradation products during the aging process of eosin-containing oil paint samples.

The combination of HRMS and Kendrick mass analysis revealed a variety of previously unreported brominated compounds, underscoring the complexity of the synthesis, drying and discoloration process of geranium lake pigments. Despite the possible differences found between the two geranium lakes studied here, Kendrick mass analysis has shown that the use of the most abundant isotope of a single tetra-brominated eosin as a base unit (R= 648.7132) facilitated the visualization of the metallic complex and the side-products generated during the synthesis. In the case of evaluating the degradation mechanism of geranium lakes over time, the use of a non-traditional Kendrick scale factor −Br+H (R=77.9105) eases the identification of the main pathways and facilitates tracking of the brominated markers in complex oil paint samples. The visible changes observed in the Kendrick plots can be confirmed by extracting the masses of these clusters and. monitoring their abundance during drying and aging. This allows us to track for first time not only the molecular changes associated to the base unit (R= 648.7132), but also to monitor the abundance of eosin-metal complexes during aging.

The results indicate that two different types of conformation, with different fragmentation patterns, could be spotted as a function of the metal used during the synthesis. Despite the possible differences found between the two metallic lakes, Kendrick mass analysis has shown that for both eosin-metal complexes, the loss of bromine begins to take place during the drying of the (linseed) oil and increases during the artificial light aging. In addition, Kendrick mass analysis facilitated the identification of other brominated species, either formed by the esterification of the carboxylate group or by fragmenting the chromophore.

The methodology developed in this study is expected to facilitate the characterization by HRMS of historical brominated pigments in a more complex matrix such as a painting. Historical paintings are highly complex mixtures containing not only pigments and oil, but preparation layers, a

mixture of different (organic and inorganic) pigments, waxes, and varnishes, among other materials added for conservation and restoration. Thus, Kendrick mass defect analysis will be used to track specific markers in samples taken from historical paintings; and the results will improve our knowledge on the possible reactions that take place during the lifetime of the painting.

ASSOCIATED CONTENT

Supporting information

The Supporting Information is available free of charge on the ACS Publications website.

Additional information on chemical structures of eosin, DI-ESI-HRMS spectra of unaged powder lakes, rescaled Kendrick plot of the lead-based eosin lake, tentative structure of the identified fragment, abundance ratio plots, DI-ESI-HRMS spectrum indicating the 2:1 complex, MS-MS spectra.

AUTHOR INFORMATION

Corresponding Author

* E-mail: Alba.AlvarezMartin@uantwerpen.be

ORCID

Alba Alvarez-Martin: 0000-0002-6756-165X

Asher G. Newsome: 0000-0003-1683-2197

Koen Janssens: 0000-0002-6752-6408

ACKNOWLEDGMENT

AAM would like to acknowledge the FWO for the international travel grant (ID K230019N). KJ and AAM also acknowledge financial support from FWO (Brussels, Belgium) through grant G054719N. This project has received funding from the European Union's Horizon 2020 research and innovation programme under grant agreement No 891714.

REFERENCES

(1) Geldof, M.; de Keijzer, M.; van Bommel, M.; Pilz, K.; Salvant, J.; van Keulen, H.; Megens, L. In *Van Gogh's Studio Practice*, Vellekoop, M.; Jansen, L.; Geldof, M.; Hendriks, H.; de Tagle, A., Eds.; Mercatorfonds, 2013.
(2) Kirby, J. In *Art of the past—sources and reconstructions, ATSR proceedings*, Clarke, M.; Townsend, J. H.; Stijnman, A., Eds.; Archetype Publications: London, 2005.
(3) Claro, A.; Melo, M. J.; Seixas de Melo, J. S.; van den Berg, K. J.; Burnstock, A.; Montague, M.; Newman, R. Identification of red colorants in van Gogh paintings and ancient Andean textiles by microspectrofluorimetry *J. Cult. Herit.* **2010**, *11*, 27-34.
(4) Anselmi, C.; Capitani, D.; Tintaru, A.; Doherty, B.; Sgamellotti, A.; Miliani, C. Beyond the color: A structural insight to eosin-based lakes *Dyes Pigm.* **2017**, *140*, 297-311.
(5) Keijzer, M. d.; Bomme, M. R. v.; Geldof, M. In *EU-Artech Symposium on Vincent van Gogh and Contemporaries*: Amsterdam, Nederland, 2009.
(6) Lee, S. H.; Nam, D. H.; Kim, J. H.; Baeg, J.-O.; Park, C. B. Eosin Y-Sensitized Artificial Photosynthesis by Highly Efficient Visible-Light-Driven Regeneration of Nicotinamide Cofactor *ChemBioChem* **2009**, *10*, 1621-1624.
(7) Yan, D.-M.; Zhao, Q.-Q.; Rao, L.; Chen, J.-R.; Xiao, W.-J. Eosin Y as a Redox Catalyst and Photosensitizer for Sequential Benzylic C−H Amination and Oxidation *Chemistry – A European Journal* **2018**, *24*, 16895-16901.
(8) Alvarez-Martin, A.; Trashin, S.; Cuykx, M.; Covaci, A.; De Wael, K.; Janssens, K. Photodegradation mechanisms and kinetics of Eosin-Y in oxic and anoxic conditions *Dyes Pigm.* **2017**, *145*, 376-384.
(9) Centeno, S. A.; Hale, C.; Carò, F.; Cesaratto, A.; Shibayama, N.; Delaney, J.; Dooley, K.; van der Snickt, G.; Janssens, K.; Stein, S. A. Van Gogh's Irises and Roses: the contribution of chemical analyses and imaging to the assessment of color changes in the red lake pigments *Herit. Sci.* **2017**, *5*, 18.
(10) Dooley, K. A.; Chieli, A.; Romani, A.; Legrand, S.; Miliani, C.; Janssens, K.; Delaney, J. K. Molecular Fluorescence Imaging Spectroscopy for Mapping Low Concentrations of Red Lake Pigments: Van Gogh's Painting The Olive Orchard *Angew. Chem. Int. Ed.* **2020**, *59*, 6046-6053.
(11) Pozzi, F.; Basso, E.; Centeno, S. A.; Smieska, L. M.; Shibayama, N.; Berns, R.; Fontanella, M.; Stringari, L. Altered identity: fleeting colors and obscured surfaces in Van Gogh's Landscapes in Paris, Arles, and Saint-Rémy *Herit. Sci.* **2021**, *9*, 15.
(12) Fieberg, J. E.; Knutås, P.; Hostettler, K.; Smith, G. D. "Paintings Fade Like Flowers": Pigment Analysis and Digital Reconstruction of a Faded Pink Lake Pigment in Vincent van Gogh's Undergrowth with Two Figures *Appl. Spectrosc.* **2017**, *71*, 794-808.

(13) Pirok, B. W. J.; Moro, G.; Meekel, N.; Berbers, S. V. J.; Schoenmakers, P. J.; van Bommel, M. R. Mapping degradation pathways of natural and synthetic dyes with LC-MS: Influence of solvent on degradation mechanisms *J. Cult. Herit.* **2019**.
(14) Sabatini, F.; Degano, I.; Colombini, M. P. Development of a method based on high-performance liquid chromatography coupled with diode array, fluorescence, and mass spectrometric detectors for the analysis of eosin at trace levels *SEPARATION SCIENCE PLUS* **2020**, *3*, 207-215.
(15) Alvarez-Martin, A.; Cleland, T. P.; Kavich, G. M.; Janssens, K.; Newsome, G. A. Rapid Evaluation of the Debromination Mechanism of Eosin in Oil Paint by Direct Analysis in Real Time and Direct Infusion-Electrospray Ionization Mass Spectrometry *Anal. Chem.* **2019**, *91*, 10856-10863.
(16) Alvarez-Martin, A.; Janssens, K. Protecting and stimulating effect on the degradation of eosin lakes. Part 1: Lead white and cobalt blue *Microchem. J.* **2018**, *141*, 51-63.
(17) Sleno, L. The use of mass defect in modern mass spectrometry *J. Mass Spectrom.* **2012**, *47*, i-i.
(18) Kendrick, E. A Mass Scale Based on CH2 = 14.0000 for High Resolution Mass Spectrometry of Organic Compounds *Anal. Chem.* **1963**, *35*, 2146-2154.
(19) Fouquet, T. N. J. The Kendrick analysis for polymer mass spectrometry *J. Mass Spectrom.* **2019**, *54*, 933-947.
(20) Ubukata, M.; Jobst, K. J.; Reiner, E. J.; Reichenbach, S. E.; Tao, Q.; Hang, J.; Wu, Z.; Dane, A. J.; Cody, R. B. Non-targeted analysis of electronics waste by comprehensive two-dimensional gas chromatography combined with high-resolution mass spectrometry: Using accurate mass information and mass defect analysis to explore the data *J. Chromatogr. A* **2015**, *1395*, 152-159.
(21) Ballesteros-Gómez, A.; Ballesteros, J.; Ortiz, X.; Jonker, W.; Helmus, R.; Jobst, K. J.; Parsons, J. R.; Reiner, E. J. Identification of Novel Brominated Compounds in Flame Retarded Plastics Containing TBBPA by Combining Isotope Pattern and Mass Defect Cluster Analysis *Environ. Sci. Tech.* **2017**, *51*, 1518-1526.
(22) Myers, A. L.; Jobst, K. J.; Mabury, S. A.; Reiner, E. J. Using mass defect plots as a discovery tool to identify novel fluoropolymer thermal decomposition products *J. Mass Spectrom.* **2014**, *49*, 291-296.
(23) Jobst, K. J.; Shen, L.; Reiner, E. J.; Taguchi, V. Y.; Helm, P. A.; McCrindle, R.; Backus, S. The use of mass defect plots for the identification of (novel) halogenated contaminants in the environment *Anal. Bioanal. Chem.* **2013**, *405*, 3289-3297.
(24) Nakamura, S.; Sato, H.; T, N. J. F. Kendrick Analysis and Complex Isotopic Patterns: A Case Study of the Compositional Analysis of Pristine and Heated Polybrominated Flame Retardants by High-Resolution MALDI Mass Spectrometry *Mass spectrometry (Tokyo, Japan)* **2020**, *9*, A0079.
(25) Sabatini, F.; Eis, E.; Degano, I.; Thoury, M.; Bonaduce, I.; Lluveras-Tenorio, A. The issue of eosin fading: A combined spectroscopic and mass spectrometric approach applied to historical lakes *Dyes Pigm.* **2020**, *180*, 108436.
(26) Vanzin, D.; Freitas, C. F.; Pellosi, D. S.; Batistela, V. R.; Machado, A. E. H.; Pontes, R. M.; Caetano, W.; Hioka, N. Experimental and computational studies of protolytic and tautomeric equilibria of Erythrosin B and Eosin Y in water/DMSO *RSC Advances* **2016**, *6*, 110312-110328.
(27) Amat-Guerri, F.; López-González, M. M. C.; Martínez-Utrilla, R.; Sastre, R. Synthesis and Spectroscopic Properties of New Rose Bengal and Eosin Y Derivatives *Dyes Pigm.* **1990**, *12*, 249-272.
(28) Arbeloa, E. M.; Previtali, C. M.; Bertolotti, S. G. Photochemical study of Eosin-Y with PAMAM dendrimers in aqueous solution *J. Lumin.* **2016**, *180*, 369-375.
(29) Seret, A.; Gandin, E.; Van De Vorst, A. Nitroxide reduction by electron transfer from the eosin triplet state: electron paramagnetic resonance and flash photolysis studies *Journal of Photochemistry* **1987**, *38*, 145-155.
(30) Kasche, V.; Lindqvist, L. TRANSIENT SPECIES IN THE PHOTOCHEMISTRY OF EOSIN* *Photochem. Photobiol.* **1965**, *4*, 923-933.
(31) Chieli, A.; Miliani, C.; Degano, I.; Sabatini, F.; Tognotti, P.; Romani, A. New insights into the fading mechanism of Geranium lake in painting matrix" *Dyes Pigm.* **2020**, *181*, 108600.